

## 3D Reflectivity-Guided Joint Migration Inversion of Multi-Well Borehole Data

El Marhfoul, Bouchaib; Verschuur, D.J.

**DOI**

[10.3997/2214-4609.201702468](https://doi.org/10.3997/2214-4609.201702468)

**Publication date**

2017

**Document Version**

Final published version

**Published in**

Proceedings of 4<sup>th</sup> EAGE Borehole Geophysics Workshop

**Citation (APA)**

El Marhfoul, B., & Verschuur, D. J. (2017). 3D Reflectivity-Guided Joint Migration Inversion of Multi-Well Borehole Data. In *Proceedings of 4<sup>th</sup> EAGE Borehole Geophysics Workshop* (pp. 1-5). Article BGP01 EAGE. <https://doi.org/10.3997/2214-4609.201702468>

**Important note**

To cite this publication, please use the final published version (if applicable). Please check the document version above.

**Copyright**

Other than for strictly personal use, it is not permitted to download, forward or distribute the text or part of it, without the consent of the author(s) and/or copyright holder(s), unless the work is under an open content license such as Creative Commons.

**Takedown policy**

Please contact us and provide details if you believe this document breaches copyrights. We will remove access to the work immediately and investigate your claim.

BGP01

## 3D Reflectivity-Guided Joint Migration Inversion of Multi-Well Borehole Data

B. El Marhfoul\* (Delft University), D.J. Verschuur (Delft University)

### Summary

---

3D borehole-related seismic data has superior quality and higher-frequency content compared to surface seismic data. These unique properties make it possible to produce high-resolution images and accurate velocity models especially around the borehole. However, using conventional imaging algorithms, that assume primary reflection energy, will retrieve only a limited area around the borehole. This problem can be overcome by including surface-related and internal multiples in the imaging algorithm to enhance the illumination of the. In addition, on-the-fly the velocity model can be updated using the so-called Joint Migration Inversion (JMI) process, which explains the full wavefield seismic data in terms of reflectivity and a propagation velocity model. To augment the results, datasets from different wells in the area can reinforce each other by simultaneous inversion to assure the consistency and improve the quality of the results. To steer and constrain the velocity estimation, the estimated reflectivity in the JMI process can be used as additional constraint for the velocity updating process.

In this paper we have deployed the full wavefield of the 3D borehole data, from two different wells, containing all orders scattering, both up- and down-going wavefields, in one integrated inversion-imaging process as proposed by the JMI methodology. The final result is a smooth accurate background velocity model along with a true amplitude reflectivity image with high resolution and maximum lateral extent.

## Introduction

In the case of datasets with sparse acquisition geometry, like 3D borehole-related seismic data, conventional imaging algorithms produce images with limited lateral extent (Blais and Hughes, 2015). Furthermore, given the poor fold distribution, no adequate update of the velocity model can be performed. The multiple scattering and the down-going wavefield are valuable signals present in the seismic data (Lee and Gou, 2016). They provide us with huge opportunities and virtues to enhance both the reflectivity image and its corresponding background velocity model on the condition that the right inversion-imaging algorithm is used (Berkhout, 2014b). Using forward modeling of the measured data based on reflectivity and propagation operators via full wavefield modeling (FWMod, Berkhout, 2014a), it is possible to derive an inversion process called JMI (Joint Migration Inversion) (Berkhout, 2014b). With JMI the involved inversion problem becomes less non-linear by decoupling propagation operators - describing the kinematics - from the scattering operators that affect the amplitudes in the seismic data. JMI applied to 3D VSP data is an extension of the full wavefield migration (FWM) algorithm for VSP data (Soni and Verschuur, 2014; El-Marhfoul and Verschuur, 2014) by including and allowing the update of the 3D velocity model. It is an iterative process, where the modeled data is constructed in a recursive manner and continuously compared with the measured input data. The residue is then translated into an update of both the reflectivity and the velocity model in a flip-flop manner. All multiples – surface and internal – are considered as part of the illuminating wavefield and are used to find reflectivity and propagation operators such that FWMod fully explains the measured data. In this way multiples do not wrongly map in the image, but will actively contribute to illuminate areas not well covered by primaries, which is particularly important for borehole data.

The output of the JMI algorithm is a smooth migration velocity model and a high-resolution reflectivity model that explain the propagation effects and all order scattering energy. Staal (2014) has already successfully demonstrated the JMI concept on 2D surface seismic data and El-Marhfoul and Verschuur (2016) for the 3D case. The significant contribution of multiple scattering and the down-going wavefield to the imaging was successfully demonstrated by El-Marhfoul and Verschuur (2015). As mentioned, in JMI the non-linearity of the inversion problem is reduced by decoupling propagation operators from the scattering operators. However, in the end these two classes of parameters are not fully decoupled: when a large reflectivity value is found, also a big change in velocity is expected. In order to steer and expedite the inversion toward a more reliable solution, the estimated reflectivity is used as additional constraint for the velocity update by imposing a penalty function within the volume that is determined by the salt structure. For surface seismic data, similar approaches for JMI were shown by Maciel et al. (2015) and Masaya and Verschuur (2016).

In this paper, using the reflectivity constraints in velocity updating, the JMI algorithm is demonstrated on the full wavefield of 3D borehole data including the down-going wavefield such that the expected value of acquiring 3D VSP data (see e.g. Gereá et al., 2016) will be even more increased.

### Joint migration inversion of 3D VSP data

With the recently developed paradigm of JMI, as explained by Berkhout (2014b), it is possible to simultaneously invert the full wavefield of the 3D borehole data, including the down-going wavefield. In the end, the same earth should explain all types of measurements. It will automatically mean that energy from multiple scattering and the down-going wavefield will be focused at the right position and, hence, will extend the lateral coverage of the image.

By using reciprocity and exchanging the sources and receivers positions in the 3D VSP data, 3D shot records are obtained, similar to surface seismic data, with the receiver depths as source elevations. In the frequency domain every ‘shot’ record number  $j$  ‘measured’ at all surface locations is then written as vector  $\vec{P}_j^-(z_0, z_{src})$ . Within JMI, in a closed-loop process, the modeled data is continuously compared to the measured data, after having updated the reflectivity and velocity model. Therefore,

the following cost-function will be minimized, based on a conjugate gradient scheme, to obtain a smooth migration velocity model (describing propagation) and a true amplitude reflectivity image:

$$J = \sum_j \sum_\omega \left\| \bar{P}_j^-(z_0, z_{src}) - \sum_m \mathbf{W}^-(z_0, z_m) \delta \bar{S}_j^-(z_m, z_{src}) \right\|^2, \quad (1)$$

with the scattered wavefield at each depth level  $z_m$  defined as

$$\delta \bar{S}_j^-(z_m, z_{src}) = \mathbf{R}^U(z_m) \bar{P}_j^+(z_m, z_{src}) + \mathbf{R}^\cap(z_m) \bar{P}_j^-(z_m, z_{src}), \quad (2)$$

where  $\bar{P}_j^+(z_m, z_{src})$  and  $\bar{P}_j^-(z_m, z_{src})$  are the incident wavefields reaching depth level  $z_m$  from above and below, respectively, from shot number  $j$ .  $\mathbf{R}^U(z_m)$  and  $\mathbf{R}^\cap(z_m)$  are the angle dependent reflectivity matrix from above and below.  $\mathbf{W}^-(z_0, z_m)$  brings the reflected wavefield from depth level  $z_m$  to the surface, where all reflection energy is observed as  $\bar{P}_j^-(z_0, z_{src})$  for ‘shot’ number  $j$  at elevation  $z_{src}$ . Note that we used the relation for transmission  $\mathbf{T}^+(z_m) = \mathbf{I} + \mathbf{R}^U(z_m)$ , which is only strictly valid for acoustic media. In the JMI approach, the incident wavefields at depth level  $z_m$  are recursively built from the original down-going source fields and the coda of multiples generated by the imaged reflectivities. Thus, the final image is reliable, laterally consistent with all types of measurements and will inherit the resolution of the data that is measured close to the reflection points.

### 3D Numerical example

In this section we will illustrate the capability of the 3D JMI algorithm in simultaneously inverting seismic datasets from different wells that are present in a certain area. In Figure 2 a), we see a display of the 3D velocity model that is selected from the 3D SEG salt model and in Figure 1 a), a cross-section of the true reflectivity model is displayed. The model covers a total area of 6 km by 6 km and a total depth of 2 km. 3D VSP seismic data was modeled, for two different wells, with a maximum frequency of 20 Hz, using reciprocity meaning that for the modeling and the imaging process the sources are assumed in the well, while the receivers were located at the surface. The 3D VSP data was modeled, for thirty-seven levels with elevation starting from  $z = 0$  m up to  $z = 1440$  m with  $\Delta z = 40$  m. The receiver grid is fixed and is densely sampled over the complete areal extent of the model according to a uniform grid with  $\Delta x = \Delta y = 20$  m.

In this numerical example, we have conducted two experiments by utilizing only dataset from well number 1 and by simultaneous inversion of both datasets from well number 1 and 2. The starting velocity model has a 1D profile, as depicted in Figure 2. In spite of the sparse acquisition geometry, at the borehole side, the 3D JMI algorithm was able to update the velocity model and steer it toward a reasonable solution. This is mainly because the multiple scattering and the down-going wavefield are reinforcing the primary energy during the inversion process. It can clearly be noticed that the JMI algorithm has succeeded in updating the velocity model even in areas beyond the coverage of primary reflections, which is due to the contribution of the multiple scattering and the down-going wavefield. Furthermore, the reflectivity constraint has helped to retrieve the main features of the salt structure, despite the poor quality of the starting model. The obtained velocity model has a smooth profile that explains the kinematics in the seismic data, Figure 2, and the high-resolution details can be found in the corresponding reflectivity model, Figure 1. Furthermore, the high angles present in the 3D borehole data make the JMI algorithm more sensitive to erroneous velocities, hence, expediting and steering the algorithm to a more accurate solution. The final estimate of the reflectivity is consistent with the true reflectivity model, within the area that is adequately illuminated by the total wavefield, and has maximum lateral coverage with a resolution that is determined by the seismic data frequency bandwidth. When both datasets are jointly inverted, the illumination is even improved which can clearly be seen in the final results of the reflectivity and velocity model. Figure 3 shows depth slices from the 3D JMI velocity cube, along the black dashed line as indicated in Figure 2 a). Note the tremendous improvement in the resolution when both datasets are simultaneously inverted.

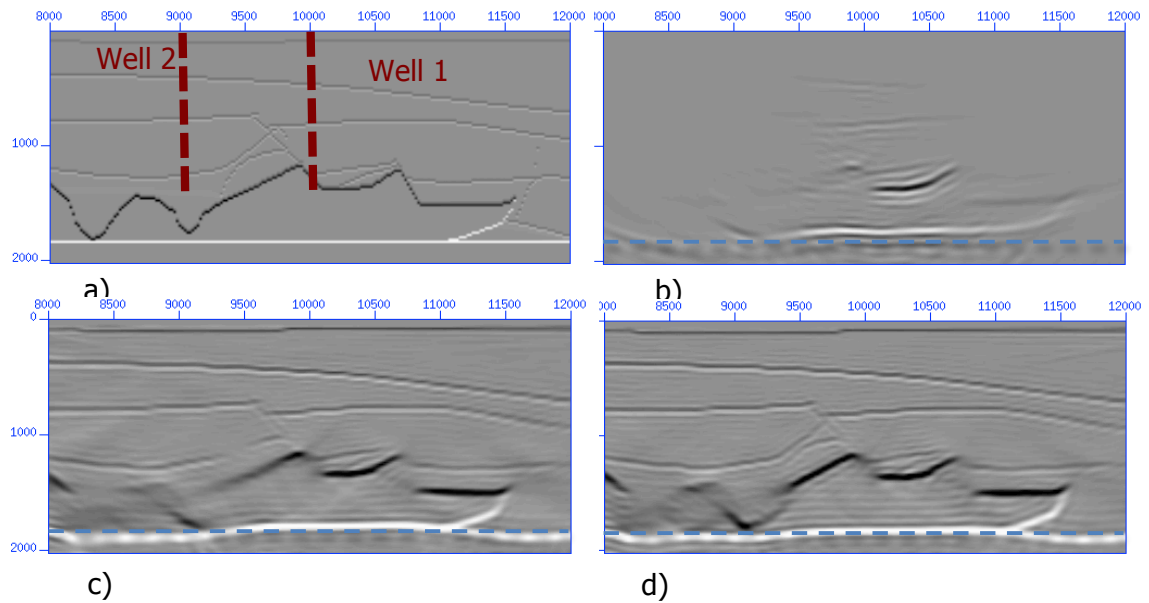


**Figure 1** Lateral cross-section from the 3D reflectivity models. a) The true reflectivity. b) PSDM image using data from well number 1. c) JMI reflectivity by utilizing data from well number 1. d) JMI reflectivity by utilizing data from well number 1 and 2 simultaneously. Note the improvements in the final images compared to conventional PSDM.

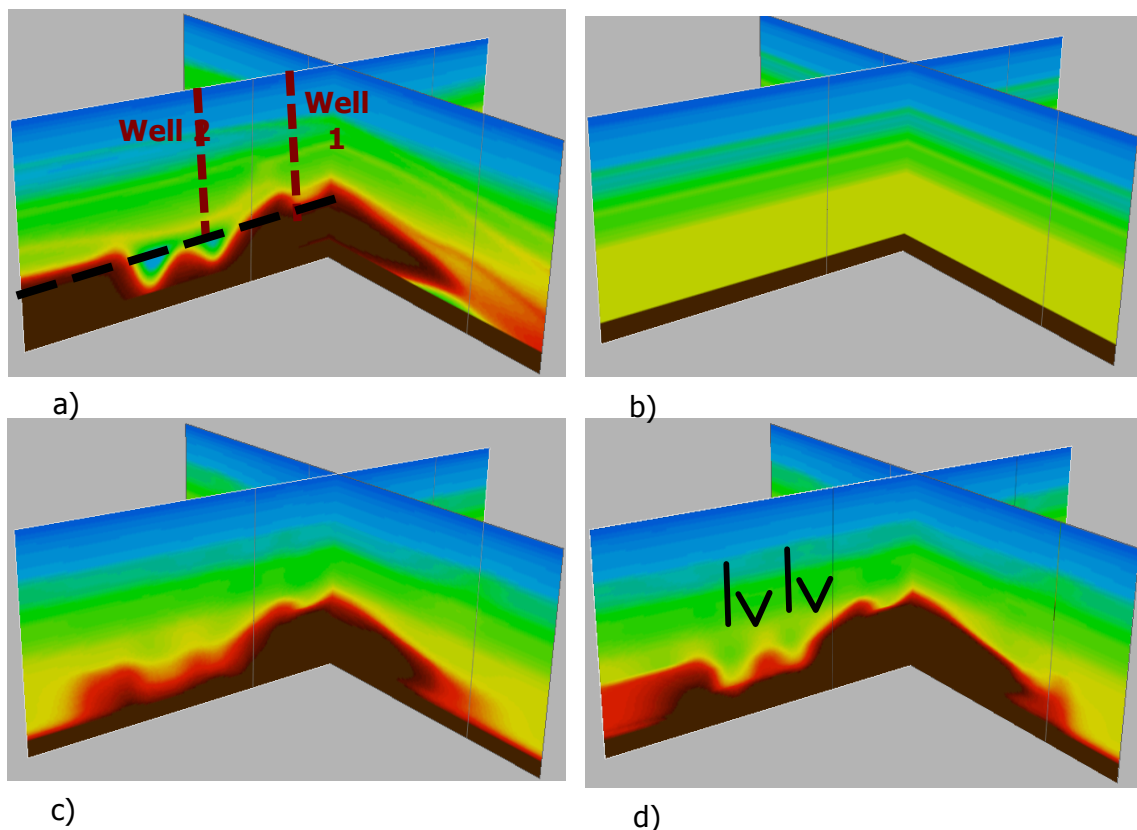


**Figure 2** 3D JMI results. a) The true velocity model. b) The starting velocity model. c) JMI estimated model by utilizing data from well number 1. d) JMI result by utilizing datasets from well number 1 and 2 simultaneously. Note the resolution increase as indicated by the black arrows.

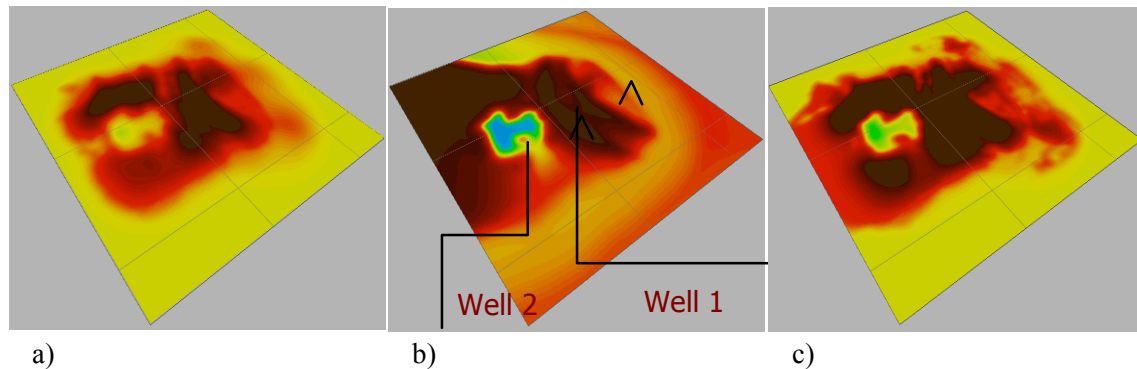


Figure 3 Depth slices from the JMI velocity models. a) By utilizing only data from well number 1. b) The true model. c) By utilizing data from well number 1 and 2 simultaneously.

## Conclusions

In this paper, the capability of the JMI algorithm in inverting datasets from multi wells is demonstrated. The full wavefield (primaries, multiples and down-going wavefield) of 3D borehole data is deployed in one integrated process. Within JMI, the modeled data is continuously compared to the measured data, after having updated the reflectivity and the velocity model. By closing the loop in the inversion-imaging process and feeding back the residual data to the JMI engine, an optimized reflectivity and velocity model will be obtained. In spite of the sparse acquisition geometry, the 3D reflectivity-guided JMI algorithm was able to provide good estimate of the velocity and reflectivity model, mainly because of the high angles available in the VSP data and the contribution from the multiple scattering and the down-going wavefield. The numerical example presented in this paper shows the effectiveness of the JMI approach, even in a complex environment, in retrieving the right kinematics properties from 3D borehole data and translate it into proper velocity update.

## Acknowledgements

The authors thank the sponsoring companies of the Delphi research consortium for their support.

## References

- Berkhout, A. J., 2014a, Review Paper: An outlook on the future of seismic imaging, Part I: Forward and reverse modelling: *Geoph.Prosp.*, **62**, 911–930.
- Berkhout, A. J., 2014b, Review Paper: An outlook on the future of seismic imaging, Part III: Joint Migration Inversion: *Geoph.Prosp.*, **62**, 950–971.
- Blias, E. and B. Hughes, 2015, 3D VSP imaging: general problems: 85th Ann. Internat. Mtg., Soc. Expl. Geophys., Expanded abstracts, 5630-5635.
- El-Marhfoul, B., and D.J. Verschuur, 2014, 3D Joint Full Wavefield Imaging of Surface and VSP Data: 84th Ann. Internat. Mtg., Soc. Expl. Geophys., Expanded abstracts, 5070-5074.
- El-Marhfoul, B., and D.J. Verschuur, 2015, 3D Full Wavefield Imaging of Up and Down-Going VSP Data: 77th Ann. Internat. Mtg., Eur. Ass. of Geosc. and Eng., Expanded abstracts.
- El-Marhfoul, B., and D.J. Verschuur, 2016, High-resolution, integrated 3D Joint Migration Inversion of Surface and VSP Data: 78th Ann. Internat. Mtg., Eur. Ass. of Geosc. and Eng., Expanded abstracts.
- Gerea, C., P.L. Pichon, G. Geddes, M. Verliac and V. Lesnikov, 2016, Proficient subsalt monitoring with 3D well seismic, deep-offshore West Africa: 86th Ann. Internat. Mtg., Soc. Expl. Geophys., Expanded abstracts, 688-692.
- Lee, C.C. and W. Gou, 2016, 3D VSP processing and imaging: a case study at Mad Dog, Gulf of Mexico: 86th Ann. Internat. Mtg., Soc. Expl. Geophys., Expanded abstracts, 5562-5566.
- Maciel, S., J. C. Costa, and D. J. Verschuur, 2015, Enhancing resolution in imaging-based velocity estimation using morphological operators: 85th Ann. Internat. Mtg., Soc. Expl. Geophys., Expanded abstracts, 5228-5232.
- Masaya S., and D. J. Verschuur, 2016, Joint migration inversion based on reflectivity-constrained velocity estimation: 86th Ann. Internat. Mtg., Soc. Expl. Geophys., Expanded abstracts, 5379-5383.
- Soni, A. K. and D.J. Verschuur, 2014, Full-wavefield migration of vertical seismic profiling data: using all multiples to extend the illumination area: *Geoph.Prosp.*, **62**, 740-759.
- Staal, X.R., D.J. Verschuur and A.J. Berkhout, 2014, Robust Velocity Estimation by Joint Migration Inversion: 76th Ann. Internat. Mtg., Eur. Ass. of Geosc. and Eng., Expanded abstracts, 4290-4295.